Optimized Structures for Photonic Quasicrystals

Mikael C. Rechtsman,[1] Hyeong-Chai Jeong,[2] Paul M. Chaikin,[3] Salvatore Torquato,[4,5,6,7] and Paul J. Steinhardt[1,6]

[1]*Department of Physics, Princeton University, Princeton, New Jersey 08544, USA*
[2]*Department of Physics, Sejong University, Gwangjin-gu, Seoul 143-747, Korea*
[3]*Department of Physics and Center for Soft Condensed Matter Research, New York University, New York 10003, USA*
[4]*Department of Chemistry, Princeton University, Princeton, New Jersey 08544, USA*
[5]*Program in Applied and Computational Mathematics and PRISM, Princeton, New Jersey 08544, USA*
[6]*Princeton Center for Theoretical Physics, Princeton, New Jersey 08544, USA*
[7]*School of Natural Sciences, Institute for Advanced Study, Princeton, New Jersey 08544, USA*

(Received 8 March 2008; revised manuscript received 27 May 2008; published 13 August 2008)

A photonic quasicrystal consists of two or more dielectric materials arranged in a quasiperiodic pattern with noncrystallographic symmetry that has a photonic band gap. We use a novel method to find the pattern with the widest TM-polarized gap for two-component materials. Patterns are obtained by computing a finite sum of density waves, assigning regions where the sum exceeds a threshold to a material with one dielectric constant, ϵ_1, and all other regions to another, ϵ_0. Compared to optimized crystals, optimized quasicrystals have larger gaps at low constrasts ϵ_1/ϵ_0 and have gaps that are much more isotropic for all contrasts. For high contrasts, optimized hexagonal crystals have the largest gaps.

DOI: 10.1103/PhysRevLett.101.073902 PACS numbers: 42.70.Qs, 61.44.Br, 71.20.−b

Photonic band gap (PBG) materials are structures composed of two or more materials with different dielectric constants arranged in a spatial configuration that forbids the propagation of electromagnetic waves in a certain frequency range. These materials may be considered the photonic analog of electronic semiconductors, and as such they have found wide technological relevance [1–3]. It has been shown recently [4–7] that quasicrystalline structures, which are not periodic but have long-range orientational order that is forbidden for periodic systems [8], are promising candidates as PBG materials. Their advantage over periodic systems in yielding a full PBG is derived from their greater rotational symmetry, as this gives rise to a more isotropic Brillouin zone (BZ) with smaller modulations that depress the gap.

Previous work on finding optimal dielectric structures [9,10] has been limited to periodic systems, where the band structure for these may be efficiently calculated numerically from a single unit cell using plane-wave expansion techniques [11]. This method is not directly applicable to quasicrystals because, by definition, they cannot be constructed from a repeating unit cell, but one can use a sequence of periodic approximants and study the limiting behavior as the cell size becomes large [12–15].

In this Letter, we apply a novel method for finding the dielectric arrangement in two-component, two-dimensional photonic quasicrystals (in the transverse magnetic–TM–polarization) that has maximal band gap. In this level set scheme, rotational symmetry may be constrained, enabling the comparison of optimal structures with different symmetries. To our knowledge, there have been no structural optimization procedures that permit this explicit constraint, making the present scheme fundamentally new. Other topology optimization schemes have been successful at finding structures that yield targeted material properties [16], but are not amenable to the constraint of rotational symmetry. We obtain optimal structures for crystals with fourfold and sixfold rotational symmetry, as well as for quasicrystals with fivefold, eightfold, and twelvefold rotational symmetry. At low dielectric contrast, the quasicrystalline structures have greater band gaps than the crystalline ones; but, at high contrasts, the sixfold (hexagonal) crystalline structures yield the greater gaps. Significantly, optimized quasicrystal gaps are more isotropic than those of crystals, for all contrasts, due to their disallowed rotational symmetries. For some applications, very isotropic band gaps may be desirable, even if the size of the full gap is slightly reduced. For example, if an application calls for a photonic structure to be surrounded by cladding of some different heterostructure (such as another photonic crystal or quasiscrystal), then it may be possible to engineer point and line defects that span larger spectral ranges and are more robust against imperfections.

In our method, the spatial configuration of the two dielectric components is expressed in terms of a finite sum of density waves $\rho(x)$, assigning regions where the sum exceeds a certain threshold a dielectric constant ε_1 and all other regions ε_0. As a practical matter, the method is most efficient if the number of density waves is small. This makes the method best suited for TM polarization for which the optimal configurations tend to have smooth features of a single length scale; by contrast, structures optimized for TE tend to have sharp features [17,18]. More specifically, the two-component dielectric function is written in terms of a function ρ such that it takes the value ε_1 when $\mathrm{Re}\{\rho\}$ is above a certain threshold and ε_0 when it is below this threshold. Thus, the dielectric constant at position $\mathbf{x}$ is given by

$$\varepsilon(\mathbf{x}) = \begin{cases} \varepsilon_1, & \text{if } \mathrm{Re}\{\rho(\mathbf{x})\} > 1, \\ \varepsilon_0, & \text{otherwise,} \end{cases} \tag{1}$$

where ρ is a sum of plane waves:

$$\rho(\mathbf{x}) = \sum_{r=1}^{R} \sum_{j=1}^{n} A_r \exp[i(\mathbf{G}_{r,j} \cdot \mathbf{x} + \phi_{r,j})], \qquad (2)$$

and A_r is the (real) amplitude of the "ring" of reciprocal-lattice vectors (defined below) indexed by r; $\mathbf{G}_{r,j}$ is the jth reciprocal-lattice vector in ring r; $\phi_{r,j}$ is the phase of the jth plane wave in ring r; R is the total number of rings employed; and the system has n-fold rotational symmetry. A ring is defined as a set of reciprocal-lattice vectors that have equal norms (for crystals) or approximately equal norms (for quasicrystal periodic approximants), and which have a predefined rotational symmetry. In particular, the rth ring with elements indexed by j and of wave number G_r is the set $\{\mathbf{G}_{r,j}: |\mathbf{G}_{r,j}| \approx G_r, \mathbf{G}_{r,j} \in \{\mathbf{G}\}\}$, where $\{\mathbf{G}\}$ is the set of reciprocal-lattice vectors. For example, the first ring of the sixfold symmetric hexagonal lattice is composed of the six nonzero reciprocal-lattice vectors closest to the origin in reciprocal space. For the case of periodic approximants, rings are chosen that approximately contain the noncrystallographic rotational symmetry in question. Thus, the closeness of the rings to shapes of true n-fold rotational symmetry defines the quality of the periodic approximant to the quasicrystal. The direct lattice vectors of the approximant unit cell are reciprocal to the primitive vectors of the reciprocal lattice. Here we have chosen $\mathrm{Re}\{\rho\} = 1$ as the threshold which divides regions with dielectric ε_0 from those of with ε_1; there is no loss of generality in this choice since selecting a different threshold is equivalent to rescaling all A_r by the same factor. The phases $\phi_{r,j}$ may be chosen to be the same for all j within ring r without loss of generality since structures are equivalent up to translations and phason shifts if the sum of their phases is equal (modulo 2π). For n even, setting equal phases $\phi_{r,j} = \bar{\phi}$ is indistinguishable from rescaling the amplitudes A_r by $\cos\bar{\phi}$; since we are allowing A_r to vary in our optimization scheme, the phases are redundant variables and can be set to zero.

In the optimization procedure, A_r and ϕ_r that maximize the full PBG between two chosen bands were found using the "steepest ascent" method (although "simulated annealing" [19] may also be used). Specifically, we iteratively adjust the amplitudes and phases A_r and ϕ_r to follow the direction of the gradient of the band gap in this parameter space. In a typical run, 5–10 rings are employed. Multiple optimizations were performed with different initial parameters in order to ensure a global maximum was reached. A key advantage of this scheme over Ref. [17] is that it allows us to find the optimum for a fixed rotational symmetry and then to study how the optimum changes with symmetry (e.g., comparing optimal configurations for a series of periodic approximants approaching an ideal quasicrystal).

For each crystal lattice, we optimize the full gap around a Bloch wave number on the order of $k = \pi/a$, where a is the lattice parameter, i.e., around the first BZ. The reciprocal-lattice points that define this BZ have wave number on the order of $2\pi/a$ and lie in a circle about $k = 0$. These are the points closest to the origin in reciprocal space with nonzero k. Consequently, the band gaps we optimize are formed by the lowest lying bands in the spectrum. For quasicrystals, the analogous reciprocal-lattice points (determined by the "quasiunit cell parameter," a) also lie in a circle about the origin, but, in principle, there is no bound to how many reciprocal-lattice points can lie inside [8]. Hence, there are infinitely many bands that lie below the complete band gap. For periodic approximants, the analogous reciprocal-lattice points form a distorted circle and there are finitely many bands below the complete band gap, with the number increasing as the periodic approximant improves (see Fig. 1). To establish convergence, we calculated the band gaps of structures with only a single ring included. As the wave number of the given ring is increased (corresponding to larger approx-

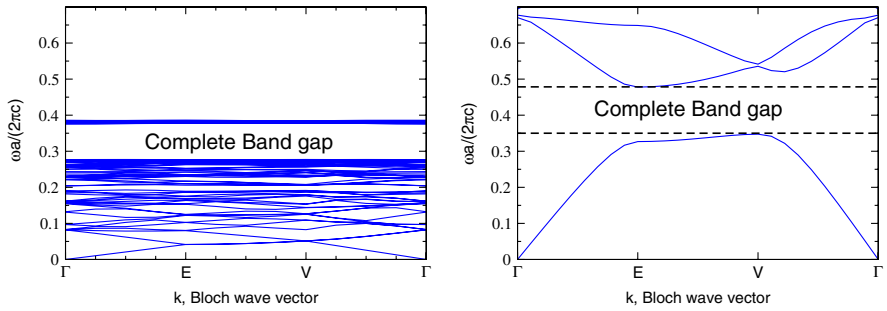

(a) fivefold (b) sixfold

FIG. 1 (color online). Band structure of the fivefold symmetric optimized structure (a) and of the sixfold symmetric optimized structure (b), both with $\varepsilon_1/\varepsilon_0 = 6$. The path traversed through the BZ is from the center (Γ) to the center of an edge (E) to a close vertex (V) and back to Γ. Here, ω is the frequency, a is the length of a quasiunit cell in (a) and a unit cell in (b), and c is the speed of light. The quasicrystal lattice parameter a is smaller by a factor of (1/8) compared to the periodic approximant unit cell. The band gap in (a) is highly isotropic as a result of the high symmetry of the structure. Here, the full gap in the sixfold case (32.5%) is larger than that in the fivefold case (30.3%) in spite of the greater isotropy of the latter.

imant cells), the value of the band gap converges to a fixed value. Note that although the quasiunit cell length has a natural definition in the Penrose tiling case (i.e., the tile side length), the dielectric functional form in Eq. (1) yields no such obvious definition. In the present case, the quasiunit cell may only be defined as a fraction of the length of the unit cell of the periodic approximant such that it characterizes the length scale of the structural features of the dielectric pattern.

Tests were performed in order to establish the accuracy of the results. For a selection of dielectric contrasts and for $n = 4$, 5, 6, 8, and 12, the number of plane waves in the diagonalization, and the number of wave vectors in the BZ were increased until convergence was achieved. Higher-order band gaps, associated with Bloch wave vectors larger than $k = \pi/a$, are not analyzed here. However, recent studies have suggested that these gaps are at most a few percent larger than the first gap [17]. Since only a finite number of rings was used in the optimization procedure, with wave numbers no more than a factor of 5 apart, structures with features on greatly different length scales cannot emerge. Optimal TM structures are of a single length scale [17], so this does not present a problem.

Optimized structures with fourfold, fivefold, and eightfold rotational symmetry are shown Fig. 2 for dielectric contrast ratio 4.0. The band structures of the optimized fivefold and sixfold configurations are shown in Fig. 1 for contrast ratio 6.0. The $n = 3$ case is not included because its optimal structures were identical to those of the sixfold case.

Optimized band gaps are plotted in Fig. 3 for each n over the contrast range 1–20. The slopes of the band gap curves form a monotonically decreasing function of the number of Bragg peaks per ring, as seen in Fig. 3 [14]. This is because the gap at the BZ edge is (to first order) proportional to the scattering amplitude across the BZ and scattering power must be spread over a higher number of peaks per ring for higher n. To understand this, consider the function ρ given in Eq. (1), with a nonzero amplitude in only a single ring and with the phases set to zero, for simplicity. If the amplitudes are defined such that the maximum value of $\mathrm{Re}\{\rho\}$ is the same for each symmetry, then clearly the scattering amplitude for a given peak decreases with n. This argument carries over (although only approximately) to the case of the dielectric function ϵ, i.e., after the cutoff has been imposed. Note that if n is even, there are n Bragg peaks per ring, but if n is odd, there are $2n$. Thus, the slopes of the fivefold structures are expected to be less than those of the eightfold structures, as seen in Fig. 3. By this reasoning, frequency gaps (stopgaps) at particular wave vectors on the BZ boundary will be larger for structures of lower symmetry. These stopgaps increase with dielectric contrast ratio.

It is clear in Fig. 3 that the higher-symmetry structures have greater gaps at low contrast [20]. The quasicrystalline structures have gaps that are more isotropic than those of the crystals for all contrasts due to the fact that their effective BZs are more circular than the BZs of crystals. For example, the BZ for sixfold symmetry is a hexagon and the effective BZ for fivefold symmetry is (approximately) a decagon. In other words, for quasicrystals, the undulations of the frequency bands (i.e., their variations as a function of wave vector) are small compared to those of crystals. Since these undulations suppress the full gap, quasicrystals have larger full gaps than crystals at low contrast. However, stopgaps at particular wave vectors increase with dielectric contrast, and crystals have larger stopgaps. Thus, crystal gaps increase more rapidly with contrast than quasicrystal gaps, and the sixfold structures have greater band gaps than any quasicrystal structure at high contrast. This is seen in Fig. 1, in which the band structure of optimized fivefold and sixfold configurations are shown at contrast 6 (where

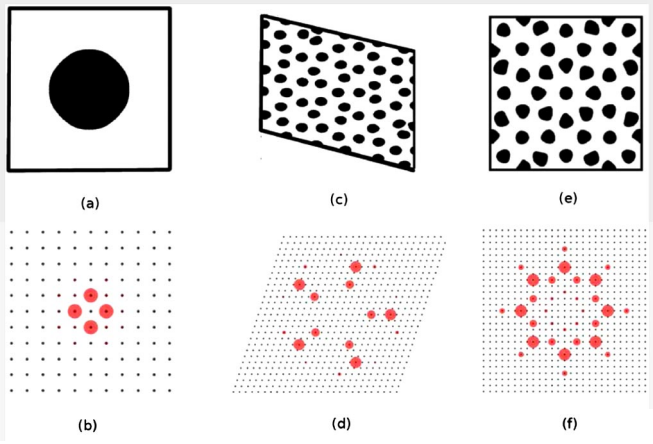

FIG. 2 (color online). Unit cells of optimized dielectric structures in the fourfold, fivefold, and eightfold rotational symmetry cases [(a), (c), and (e), respectively], with $\varepsilon_1/\varepsilon_0 = 4.0$. In (b), (d), and (f), the grid points indicate the reciprocal lattice of the fourfold, fivefold, and eightfold unit cells. The red (or gray) circles indicate the rings and have radii proportional to $|A_r|$.

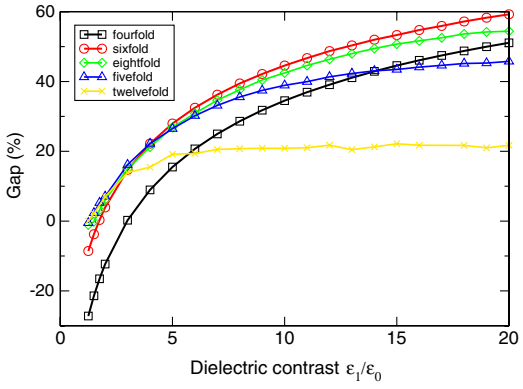

FIG. 3 (color online). Normalized band gaps of optimized density wave structures for rotational symmetries $n = 4$, 5, 6, 8, and 12 as a function of the dielectric contrast of the two phases. For reasons discussed in the text, structures of high symmetry tend to have larger band gaps for low contrast, but smaller gaps for high contrast.

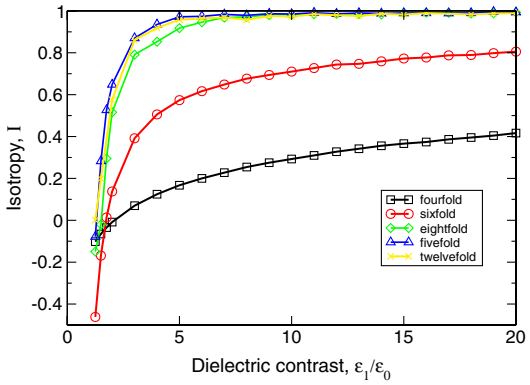

FIG. 4 (color online). The degree of isotropy, $\mathcal{I}$ (defined in the text), of the optimized dielectric configurations, plotted against dielectric contrast. The quantity $\mathcal{I}$ is bounded from below by -1 (for the case of a homogeneous medium) and from above by 1 (for the case where the upper and lower bands are perfectly flat). For all contrasts, quasicrystalline structures have higher isotropy. Note that the fivefold case has greater isotropy than the eightfold case because the former has an effective BZ that is closer to a circle than that of the latter. These zones are a decagon and an octagon, respectively.

the sixfold has the greater gap). At roughly contrast 20, the eightfold and fourfold cases meet. Although this suggests that the fourfold structure has a larger band gap than the eightfold, they remain too close at higher contrasts to distinguish.

As mentioned it may be useful to have more isotropic gaps, even at the cost of a few percent in the full gap width. We define a measure of isotropy for a PBG as

$$\mathcal{I} = \frac{\min_{\mathbf{k},\mathrm{EBZ}}\{\omega_h(\mathbf{k})\} - \max_{\mathbf{k},\mathrm{EBZ}}\{\omega_l(\mathbf{k})\}}{\max_{\mathbf{k},\mathrm{EBZ}}\{\omega_h(\mathbf{k})\} - \min_{\mathbf{k},\mathrm{EBZ}}\{\omega_l(\mathbf{k})\}}, \tag{3}$$

where the minima and maxima are taken over all $\mathbf{k}$ on the boundary of the effective BZ (EBZ), and ω_l and ω_h are bands just below and just above the gap. It is clear from its definition that $\mathcal{I} \in [-1, 1]$. When $\mathcal{I}$ is at its greatest, the gap is perfectly isotropic, and it is at its lowest in a homogeneous material. Isotropy is plotted against dielectric contrast for all rotational symmetries in Fig. 4. The quasicrystals all have higher isotropies than the crystals. $\mathcal{I}$ increases monotonically as the EBZ becomes more circular. In particular, for the eightfold, tenfold, and twelvefold cases, the EBZs are an octagon, a decagon, and a dodecagon, respectively. The isotropy of the twelvefold optimized band gap is indistinguishable from that of the fivefold, suggesting that the isotropy reached saturation.

In conclusion, we devised a scheme to find crystalline and quasicrystalline dielectric structures that maximize the PBG in two dimensions. Because of their high, noncrystallographic rotational symmetries, quasicrystals may have highly isotropic gaps that are larger than those of crystals at low dielectric contrasts. However, for sufficiently high contrasts, optimized hexagonal crystals have greater gaps. Thus, photonic quasicrystals may be well suited for use when band gap isotropy is of importance. A future challenge is to optimize three-dimensional photonic quasicrystals. The intuition gained from studying the two-dimensional case, generalized to three dimensions, may lead to photonic quasicrystal structures with large three-dimensional gaps.

We thank Marian Florescu and Weining Man for helpful discussion. S. T. thanks the Institute for Advanced Study for its hospitality during his stay there. This work was supported by the National Science Foundation under Grant No. DMR-0606415 and the Korea Science and Engineering Foundation (KOSEF) under Grand No. R01-2007-000-11388-0. M. C. R. acknowledges the support of the Natural Sciences and Engineering Research Council of Canada.

[1] E. Yablonovitch, Phys. Rev. Lett. **58**, 2059 (1987).
[2] S. John, Phys. Rev. Lett. **58**, 2486 (1987).
[3] J. D. Joannopoulos, P. R. Villeneuve, and S. Fan, Solid State Commun. **102**, 165 (1997).
[4] M. E. Zoorob, M. D. Charlton, G. J. Parker, J. J. Baumberg, and M. C. Netti, Nature (London) **404**, 740 (2000).
[5] X. Zhang, Z. Q. Zhang, and C. T. Chan, Phys. Rev. B **63**, 081105(R) (2001).
[6] L. Dal Negro, C. J. Oton, Z. Gaburro, L. Pavesi, P. Johnson, A. Lagendijk, R. Righini, M. Colocci, and D. S. Wiersma, Phys. Rev. Lett. **90**, 055501 (2003).
[7] W. Man, M. Megens, P. J. Steinhardt, and P. M. Chaikin, Nature (London) **436**, 993 (2005).
[8] D. Levine and P. J. Steinhardt, Phys. Rev. B **34**, 596 (1986).
[9] M. Burger, S. J. Osher, and E. Yablonovitch, IEICE Trans. Electron. **E-87-C**, 258 (2004).
[10] M. Maldovan, C. K. Ullal, W. C. Carter, and E. L. Thomas, Nature Mater. **2**, 664 (2003).
[11] R. D. Meade, A. M. Rappe, K. D. Brommer, J. D. Joannopoulos, and O. L. Alerhand, Phys. Rev. B **48**, 8434 (1993).
[12] K. Wang, S. David, A. Chelnokov, and J. M. Lourtioz, J. Mod. Opt. **50**, 2095 (2003).
[13] W. Steurer and D. Sutter-Widmer, J. Phys. D **40**, R229 (2007).
[14] P. N. Dyachenko and Y. V. Mikyaev, Proc. SPIE Int. Soc. Opt. Eng. **6182**, 61822I (2006).
[15] P. N. Dyachenko, Y. V. Mikyaev, and V. E. Dmitrienko, JETP Lett. **86**, 240 (2007).
[16] S. Torquato, S. Hyun, and A. Donev, Phys. Rev. Lett. **89**, 266601 (2002).
[17] C. Y. Kao, S. Osher, and E. Yablonovitch, Appl. Phys. B **81**, 235 (2005).
[18] O. Sigmund and K. Hougaard, Phys. Rev. Lett. **100**, 153904 (2008).
[19] S. Kirkpatrick, C. D. Gelatt, Jr., and M. P. Vecchi, Science **220**, 671 (1983).
[20] It has been conjectured that the structure with the largest TM-band gap consists of a triangular lattice of circular inclusions [18]. Our results show that, at low dielectric contrast, there exist quasicrystal structures with larger band gaps. At sufficiently high contrast, though, the lattice conjectured in [18] becomes optimal.